A Surface View of Etching

Experiments conducted with scanning tunneling microscopes in ultrahigh vacuum reveal a fascinating, step-by-step picture of the etching process.

John J. Boland and John H. Weaver

Chemical etching has been practiced since at least the late Middle Ages. In its early form, it involved coating an object, such as a metal plate, with wax, carefully patterning the hardened wax by cutting down through it with a sharpened tool to expose but not penetrate the object's surface and then exposing the object to an etching solution, typically an acid. With time, the etchant molecules in the solution would react with atoms of the exposed surface to form reaction products that would dissolve, thereby removing material from the surface.

A time-consuming task, precision etching was once the exclusive domain of craftsmen and artists who advanced their skills through trial and error, rather than by grappling with the science involved. It is only relatively recently that, say, the etching of copper by nitric acid has been described by a chemical equation, and even more recently that concepts associated with crystal surfaces and reaction pathways have been applied to etching.

Although much has changed in the last several centuries, the basic ingredients of etching have remained the same. We still have surfaces on which etchant atoms or molecules adsorb and we still have changes in the structure of the surface when the etch products are removed. In the high-output technologies of today—such as those that produce integrated circuits and semiconductor-based devices—wax has been dispensed with in favor of chemical resists that can be patterned by exposure to light, and one-of-a-kind art has been replaced by automated tools that repeatedly etch patterns with submicrometer dimensions and high aspect ratios.[1]

Today, chemical etching is the cornerstone of many industries. The $700-billion-a-year US microelectronics industry, for one, would not exist without processes for forming precise geometrical structures with specific chemical and physical properties.

Not confined to high technology, etching is often used when inexpensive pattern formation is required. It plays an essential role in our everyday lives, being an integral part of the processes used to provide us with, say, the books we read (offset printing) and the coins we spend or save.

The modern industrial concept of chemical etching now also includes dry etching, in which the surface is exposed to gaseous molecules, rather than to liquids, and the etch products are desorbed into the vapor. Since desorption requires energy to break surface bonds, temperatures as high as 900 K may be needed. In many cases, therefore, it is advantageous to alter the surface chemistry and enhance the formation of volatile species. Numerous so-called assisted etching techniques have been developed to increase etching rates, to achieve directed or anisotropic etching and to make etching possible, at reduced temperatures, for even the most inert materials.

Despite chemical etching's long history and enormous economic value, the detailed mechanisms behind the technique are only now being uncovered—thanks, in part, to the development of scanning tunneling microscopy (STM), which can reveal chemical reactions and surface structures with atom-scale precision.[2] Although we cannot yet follow etching in real time with STM, we can certainly investigate how etching depends on the temperature, flux and fluence of the etchant gas. And if we analyze changes in surface morphology that accompany etching and the rates at which they occur, we can determine how the atomic structure of the surface governs the energy barriers for product desorption.

So far, thermally activated etching of single-element[3,4] and compound semiconductors[5] has been successfully studied with STM. Related studies have emphasized other key components in real-life etching—namely, those associated with the physical impact of energetic ions (sputtering)[6] and irradiation by photons (photochemistry and photon stimulated atom desorption).[7]

The ultimate goal is to formulate a more comprehensive picture of semiconductor etching by combining the results of studies of surface morphologies with insights gained from theory or modeling and from a host of other probes of surface reactions. Although the picture is far from complete, enough details have been established to paint an impressionist view of chemical etching.

The etching arena

Ideally, an experiment that seeks to probe etching on the atomic scale would begin with a clean surface. In the real world, however, even clean surfaces are marred by structural imperfections on the same atomic scale. Figure 1a depicts several kinds of atomic-scale imperfection—namely, steps, vacancies and pits.

Steps are always present because surfaces are never atomically flat over large dimensions. When a real surface is exposed to a chemical etchant, the incident molecules

JOHN BOLAND *is in the department of chemistry at the University of North Carolina at Chapel Hill.*
JOHN WEAVER *is in the department of chemical engineering and materials science at the University of Minnesota in Minneapolis.*

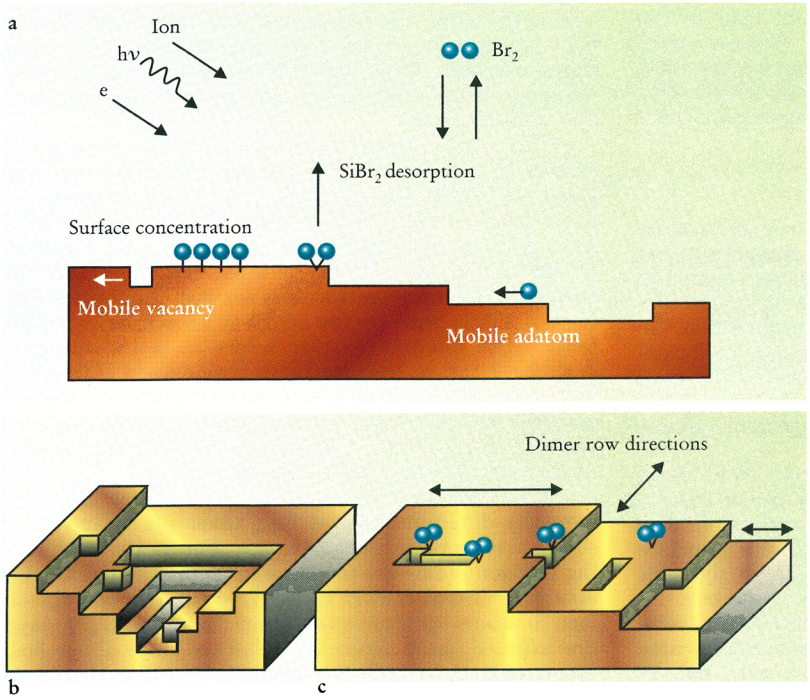

FIGURE 1. SCHEMATIC VIEWS of etching, starting with a silicon (100) surface being exposed primarily to bromine molecules, but also to electrons, photons and ions (**a**), as is often the case in real-world etching. A nanometer-sized observer standing on the top terrace would see a clean surface with steps that lead down to the bottom terrace, which is occupied by a wide pit. If the temperature were raised and etching started, the observer would also see the vacancy on the top terrace move around, the steps ebb and flow across the surface and halogen adatoms that jump about the surface according to Boltzmann statistics. As the etching proceeded, the nano-observer would see the surface become either deeply indented (**b**), or more regular (**c**), depending on the relative energy barriers for desorption at the different surface sites.

probe the potential energies of the different surface sites they encounter. For instance, halogen molecules (the principal etchants used in dry etching) that impinge on silicon at room temperature break up into atoms, which then form strong chemical bonds with the dangling bonds of the Si surface atoms.

At room temperature, the accumulating halogens passivate the surface by tying up the dangling Si bonds, thereby rendering the surface chemically inert. But at higher temperatures, the action and structures on the surface become more dynamic. With enough energy, a bromine atom can jump from one site to another. Holding it back is a diffusion barrier whose height depends on the jump direction and whether the Br atom jumps between identical sites on a terrace or between terrace sites and step sites—as can be envisioned from figure 1.

For example, a halogen atom on a clean Si(100) terrace finds barriers of about 1 eV, which it can hop over about 10^7 times per second at 900 K. (See the box on page 36 for a short tutorial on silicon's crystalline structure.) At this temperature, atoms that are intrinsic to the surface can also move, so that a Si atom at a step can move onto a terrace and vice versa.

Thermal activation also accounts for the formation and diffusion of vacancies on terraces. At 900 K, the Br atoms on the surface can form silicon dibromide ($SiBr_2$) units that can desorb, following a sequence of events described below. Desorption frees up space for incoming molecules, and the process continues.

What controls the surface morphology?

One could presume that a surface exposed to an etchant would quickly become too rough for an STM probe to distinguish atomic order—like the deeply and irregularly etched surface depicted schematically in figure 1b. It turns out, however, that changes in surface morphology can be controlled by exploiting how reaction rates differ at the various kinds of surface features. By investigating these changes, we ask how much one pathway is favored over another. As we will see, the differences in the energy barrier can be as little as 0.1 eV—small compared to the 3 eV barrier for $SiBr_2$ desorption, but sufficient to make possible the controlled evolution of the surface morphology (and its study with STM).

Figure 1c shows schematically how site-to-site variations influence surface morphology. The example is the surface of Si(100), but experiments and modeling have demonstrated that the layer-by-layer removal pattern depicted in the figure also applies to Si(111) and gallium arsenide (110) surfaces.[3–5]

In the case of Si(100), atoms of the exposed surface form dimers that align along the [011] direction. On the top terrace, etching has created a chain of vacancies (missing dimers) that extends along that terrace's [011] direction. The dimer row direction rotates by 90° at each step because of the structure of Si's diamond lattice. This intrinsic structural property engenders a surface anisotropy that is reflected in the diffusion of adatoms and vacancies over the surface, and, ultimately, in the etching pattern itself—shown dramatically in figure 2.

Terrace pitting disrupts the local surface bonding and leaves the surface atoms in a variety of different bonding sites, each with its own barrier for desorption of $SiBr_2$. Desorption from sites at the end of a pit leads to pit elongation, whereas removal from a side site produces a branch—as sketched in figure 1c. Steps have different desorption barriers, which depend on whether a site is near a kink (as sketched in figure 1c) or not. Terraces offer the largest number of etching sites, but Si atoms on terraces, being the most tightly bound, have the highest desorption barrier. Again, the consequences of this contrast are manifest in the etching patterns—see figure 2.

Our picture of etching controlled by desorption barriers assumes that halogens can discriminate among different sites. But this is not always the case. Fluorine atoms are small, and their reaction with silicon atoms is so exothermic that they can insert directly into bulk Si–Si bonds, even at room temperature. This extreme reactivity

and lack of chemical discrimination could lead to the severe roughening suggested in figure 1b. However, such deep insertion is unlikely for chlorine, bromine and iodine, to which our desorption barrier picture is applicable. This article focuses on Br etching because it represents these less reactive halogens.

Surface reconstruction

If one examines semiconductor surfaces in a little more detail than offered in figure 1, one soon recognizes that atoms on surfaces can change their positions relative to what would be expected if the crystalline structure continued unchanged to the surface—"bulk termination," in surface science parlance. These rearrangements ("reconstructions" is the technical term) are driven by the need to minimize the surface energy. For semiconductors, dangling bonds cost energy and their rearrangement reduces the energy bill.

In the case of Si(100), each exposed atom should have two dangling bonds, but, with small shifts, the atoms can pair up to form dimers. In this "2×1 reconstruction," two of the dangling bonds have been converted into a surface dimer bond.[8] The dimer atoms also undergo dynamic buckling at room temperature—as shown in the box.

The Si(111) surface rearranges the lattice over several layers and adopts a 7×7 reconstruction. This complicated structure, which took many years to sort out,[9] has 19 dangling bonds per unit cell, compared to 49 bonds in an unreconstructed cell of the same size. In the top layer, where the atom density is not very high, each Si atom has one dangling bond that extends into the vacuum. Since electrons from the STM tip can tunnel into this dangling bond, STM images can capture the structure of this adatom layer.

The 7×7 reconstruction even extends beneath the surface to include a second Si layer called the rest layer. Here, we find triangle-shaped arrays of silicon atoms that are arranged locally within the usual Si bulk structure. Each array is separated from the next by a bordering row of silicon dimers, similar to those found on the (100) surface. However, on the (111) surface, the dimers introduce a subtle shift in the registry, known as a stacking fault. The dimer rows also intersect at the corners of each 7×7 cell to produce holes that extend through the top surface layer. Wonderfully complex, the reconstructed surface presents a variety of sites for reaction with incident halogen molecules, making it an invaluable platform for testing models of chemical etching.

The ways in which surfaces reconstruct are fundamentally different when etching takes place, and not all surfaces respond in the same way. For Si(100), the reacting halogen atoms are too large to fix or stabilize the bulk structure of each newly exposed layer. Instead, the surface Si atoms spontaneously dimerize as successive layers are exposed, as in figure 1c. Since surface dimer bonds are weaker than bulk Si–Si bonds, this dimerization actually facilitates further etching.

Si(111) is dramatically different, for halogen atoms

Silicon's (100) and (111) Surfaces

Crystalline silicon arranges itself in a tetrahedral diamond structure, like its fellow group IV element carbon. Inside this structure are regular planes of atoms, which are conventionally designated by the directions of their normals with respect to the unit cell. As can be seen in the figure to the right, silicon's densest plane is (111). The (100) plane is significantly less dense.

To minimize their energy, surface atoms spontaneously reconstruct the way in which they are bound to their neighbors, as shown in the figure on the lower right. For example, without reconstruction, the atoms closest to the Si(100) surface (shown here in red) would be bound only to atoms in the layer immediately below (blue). Lower in energy and, hence, more favorable, is the reconstructed 2×1 surface, on which the uppermost atoms form rows of dimer pairs.

The figure below shows the complex reconstructed 7×7 surface of Si(111) before and after etching has removed the sparse top layer of Si adatoms (shown in red on the left) and has replaced them with halogen atoms (shown in yellow on the right). The right-hand part of the diagram illustrates how the dimerization of the second, rest layer alters the registry of the first and third layers. On the faulted side, the atoms in the first layer lie directly above those in the third layer. On the unfaulted side, the two layers are shifted.

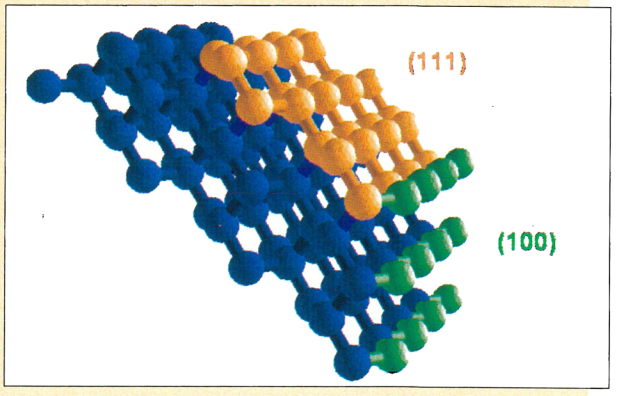

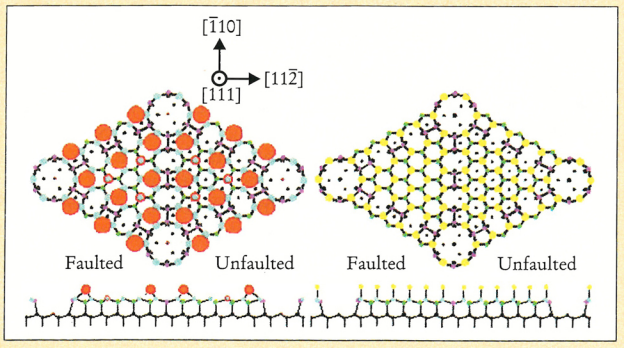

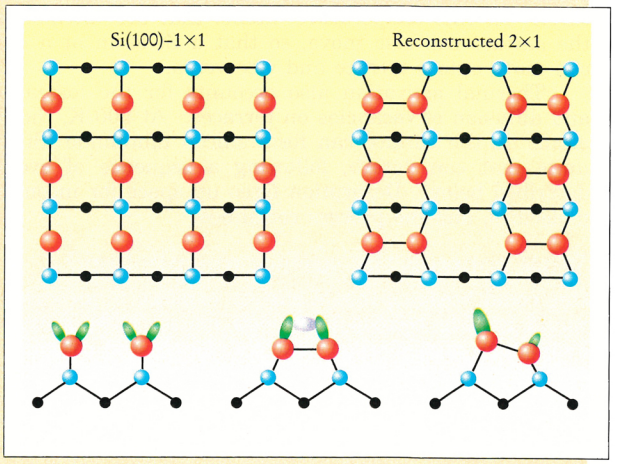

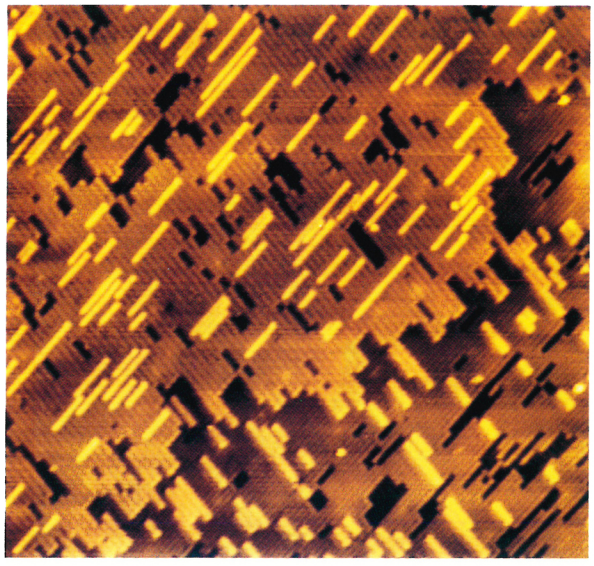

FIGURE 2. EXPOSING A SILICON (100) SURFACE to molecular bromine at 800 K roughens the profile of intrinsic steps, as shown in this scanning tunneling microscope image. Elongated along the dimer row directions (which rotate by 90° at each step) are dark areas that represent pits one atom layer deep. The bright lines that run perpendicular to the pits are silicon dimer chains that have grown on the terraces and whose supply of Si comes from atoms released from terrace and step sites during etching. These patterns reflect the energies of desorption of silicon dibromide at the different sites of the surface. The area shown in the figure measures 55 × 55 nm.

can easily stabilize its exposed bulk structure. In this case, etching requires halogen atoms to be inserted into strong Si–Si bonds. Since the barrier for this insertion is large, etching is expected to be slower. Here, the halogen etchants play two roles. First, they remove Si. Second, they tie up the dangling bonds of the bulk-terminated surface, thereby eliminating the driving force for reconstruction. In this second role, then, the halogen atoms keep the surface from reconstructing, but make etching harder.

Etching Si(111)

Keeping in mind the importance of surface features and reconstruction, we now turn to look at how the etching of Si(111) actually proceeds on the atomic scale.

Though complex, the arrangement of the various kinds of site on the Si(111) surface is ordered—a property that makes it possible to study Si(111). In fact, we can turn this complexity to our advantage by using halogen molecules as probes of the different sites. In common with the artificial surface shown in figure 1, the Si(111) surface offers sites with different desorption barriers, but now it is the 7 × 7 reconstruction itself—rather than a cartoonist—that provides the variety of sites.

Site-to-site variations are seen most dramatically in the outermost layer of Si adatoms, whose open, loose structure is especially vulnerable to attack by halogen molecules—so much so that the Si adatoms can be completely stripped from the surface while leaving the rest of the surface structure intact. Figures 3a and 3b show the reconstructed surface before and after adatom removal, respectively.[10] The stacking faults introduced into the rest layer by the dimer rows are now clearly evident in figure 3b: The bright triangular arrays are faulted, whereas the darker arrays are not.

The (111) surface not only makes it possible to study the selective etching of Si atoms in different settings, but also provides insight into how such behavior can be exploited for future applications. Selective etching is possible because weakly bonded Si atoms, such as those in the adatom layer, have smaller energy barriers for halogen insertion, so reaction occurs at lower temperatures. Under the conditions captured in figure 3b, the energy barrier for inserting halogen atoms into the dimer and bulk bonds of the rest layer are much too large to yield measurable desorption rates.

The exposed Si(111) rest layer does not remain dormant indefinitely. At modest temperatures (700 K and below), little real etching occurs, but, even so, the rest layer changes structure in response to the presence of halogen atoms. A key aspect of this change is the formation of bulk-terminated surface domains that are stabilized by halogen atoms. To accomplish this stabilization, Si atoms must be found to fill the holes of the original rest layer. Since the supply of atoms is readiest at steps, bulk domains tend to nucleate near step edges.

These dynamical changes are not limited to terrace sites. Steps, too, change their structure in response to the newly formed bulk domains. On the unetched 7 × 7 surface, steps meander with no apparent or preferred direction, but this wandering changes dramatically once bulk domains begin to form.[11]

For steps that have their outward normals pointing in what we will call the A direction (see figure 4), the bulk structure exists right up to the edge. However, for B-type steps, triangular stacking-fault structures are always found. Remarkably—as can easily be seen in figure 4—both types of step have the same edge structure. In fact, the only difference is the presence of faulted structures along the B-type steps. Stacking faults like these cost energy, which increases their energy relative to A-type steps. This transformation of both terrace and step sites sets the stage for, and heralds the commencement of, full-scale Si(111) etching.

The contrast in reaction sites becomes manifest in the etching profile. In the hierarchy of binding sites, Si atoms at A-type steps are more tightly bound than those at B-type steps. This step energy difference comes immediately into play when the temperature is high enough to promote desorption from steps. Under steady-state exposure, A-type steps tend to be smooth, whereas B-type steps have a jagged sawtooth appearance.[12] This difference can be understood in terms of step energies. Kink formation along an A-type step results in segments of higher energy B-type steps. On the other hand, the roughening of B-type steps is favored and creates short lengths of lower-energy A-type steps. This roughening occurs because the stacking-fault structures at B-type steps are bordered by weakly bonded Si dimers, which are preferentially etched.

As it continues, this process eventually undercuts the entire faulted region, resulting in the formation of the jagged step edge shown in figure 4. Again, we see etch features and shapes that reflect differences in Si bond strengths and the distribution of these bonds on the surface.

Since they are the most tightly bound, the Si atoms at terrace sites are removed last. Their removal seems to be initiated by reaction of halogen atoms with triangular

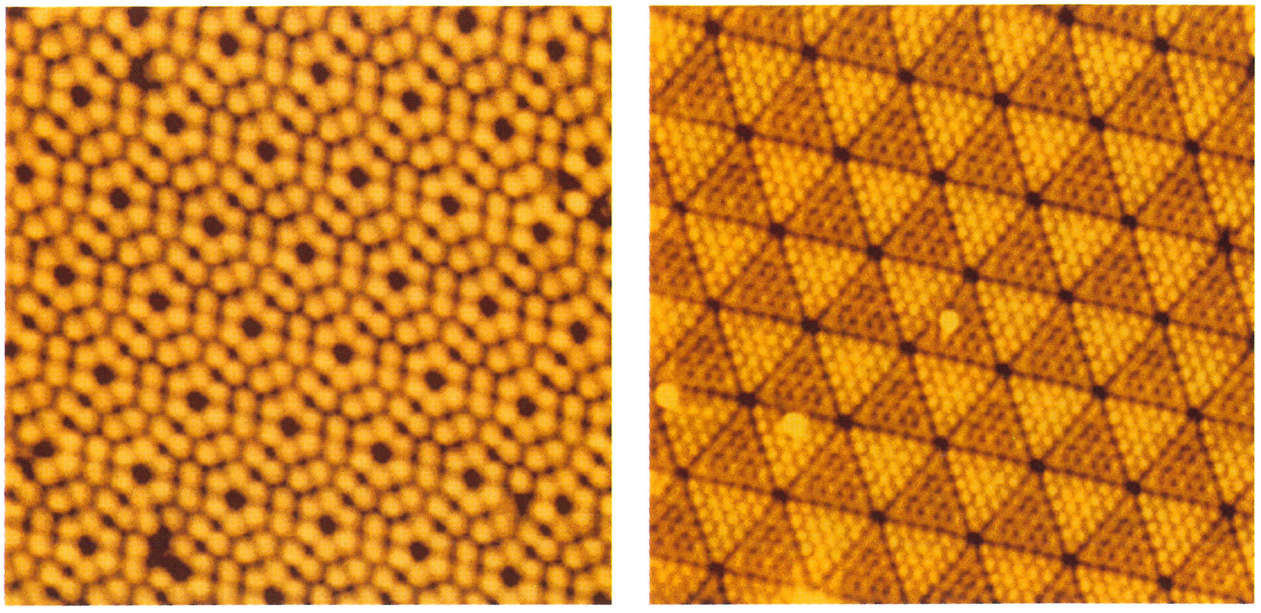

FIGURE 3. BEFORE AND AFTER the removal of adatoms from a reconstructed 7×7 silicon (111) surface as imaged by a scanning tunneling microscope. **a:** The adatom layer of the clean Si(111) 7×7 surface. **b:** The rest layer following removal of the adatom layer in **a** by bromine etching at 675 K. The three pale features are adatoms that remained on the surface. Layer-specific removal like this reflects the lower bonding strength of the Si adatoms in the top layer compared to the Si atoms in the rest layer. The area shown in both figures measures 17×17 nm.

stacking-fault structures present on these terraces. Evidence for this process is found in the faulted structures often seen at the bottom of etch pits. Such features must form spontaneously whenever a new layer is exposed. Where could they come from?

The answer may lie in a recently developed model that describes triangular stacking-fault structures as ordered vacancies.[13] In this scenario, the high-temperature surface is exceptionally dynamic and contains numerous vacancies, created either thermally or by isolated etching events. These vacancies may then arrange themselves to form faulted structures, which are subsequently etched to produce triangular pits. The rules that govern the lateral growth of these pits are exactly those that control etching at surface steps. Growth ultimately produces large triangular etch pits (see figure 5), whose shapes are determined by the stability of the type-A steps that form the perimeter of the pits.

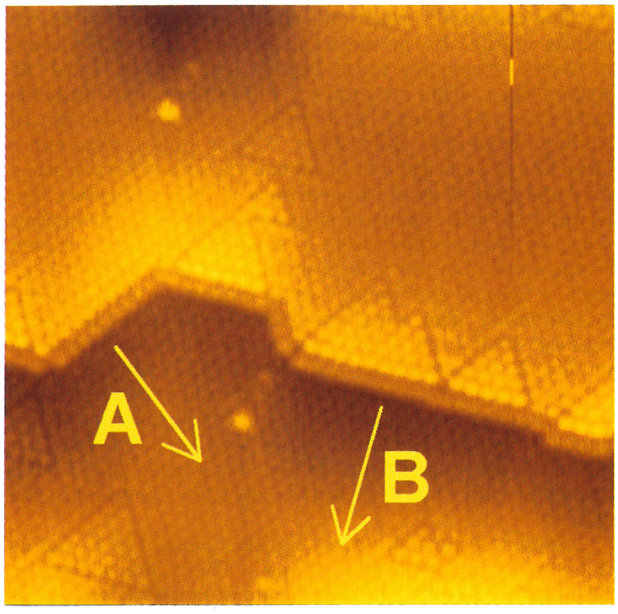

FIGURE 4. TYPE-A AND TYPE-B STEPS on a bulk-terminated Si(111) 1×1 surface. This scanning tunneling microscope image shows that the two types of step have the same step-edge structure. For type-A steps, the bulk 1×1 structure extends right up to the step whereas the upper terraces for type-B steps are dressed with triangular stacking-fault structures. The area shown in the figure measures 16.5×16.5 nm.

Etching Si(100)

Having focused on the complex, reconstructed Si(111) surface to show how surface morphology both controls and is controlled by etching, we now turn to the simpler Si(100) surface to investigate the sequence of atomic events that lead to desorption and to determine the relative energies that give rise to the various etch patterns that are formed. To visualize the etching of the reconstructed Si(100) 2×1 surface, we must continue to keep in mind how dynamic the etching arena is. Desorption events occur while halogen and Si atoms move around on terraces, while vacancies move within the surface layer and while steps move across the surface. As in the case of Si(111), these processes depend on temperature, the local structure and the halogen composition.

The Si(100) surface depicted in figure 2 was imaged at room temperature after etching with Br_2 gas at 800 K. How much Br is on this surface (90% of a monolayer, in

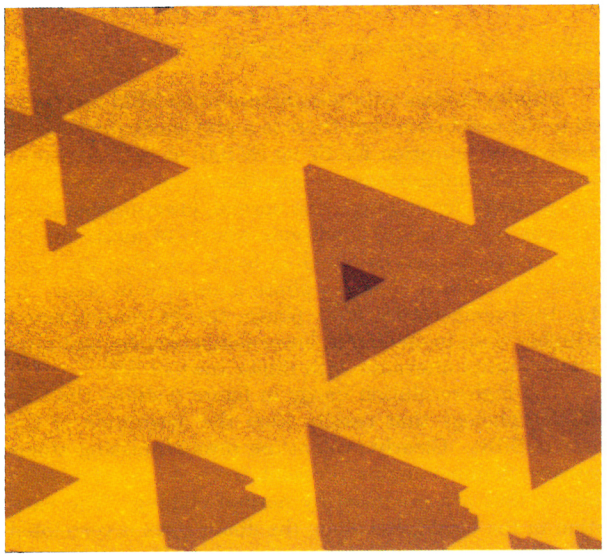

FIGURE 5. TERRACE PIT MORPHOLOGY on the Si(111) surface. As seen in this scanning tunneling microscope image, etch pits are typically triangular and enclosed by low-energy type-A steps. In instances where there are deviations from this perfect structure, short sections of higher-energy type-B steps are incorporated along the step perimeter, which drives the formation of triangular etch pits. The area shown in the figure measures 150 × 150 nm.

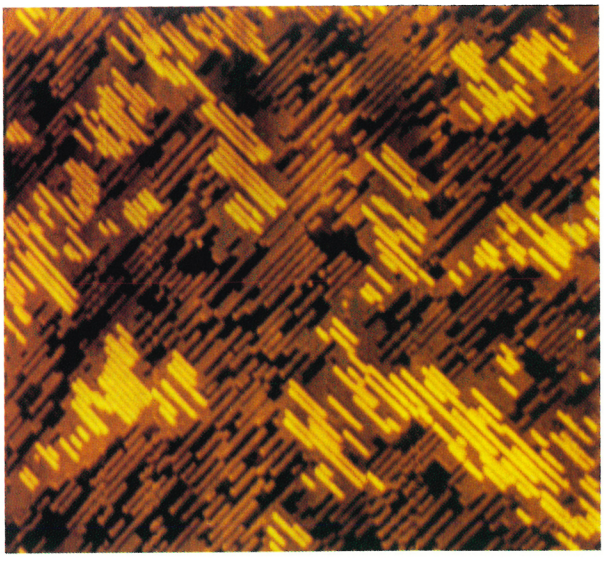

FIGURE 6. EXPOSURE OF SILICON (100) to molecular bromine at 900 K results in a phase transformation for the adsorbed Br that establishes rows of Si atoms with two Br adatoms separated by rows with only one adatom. The desorption of the volatile $SiBr_2$ molecules results in rows of missing atoms that are separated by dimer chains. Also evident in this scanning tunneling microscope image are vacancy rows derived from dimers, as is the case for etching under conditions of lower surface concentration. The area shown in the figure measures 60 × 60 nm.

fact) can be determined by imaging at different tip biases. In the area shown, a ragged step separates terraces whose dimer rows change direction by 90°. Elongated along the dimer row directions are dark areas that represent pits one atom layer deep. The bright lines that run perpendicular to those pits are Si dimer chains that have grown on the terraces and whose supply of Si comes from atoms released from terrace and step sites during etching.

With STM, not only can we see the results of desorption, but we can also deduce the sequence of events that lead to it. Desorption is generally thought to start from a configuration in which one Br adatom is bonded to each Si atom of a surface dimer. To transfer a Br atom from one Si atom to its partner, the dimer bond between the surface pair has to be broken. This action costs energy, but prepares a $SiBr_2$ unit that can attempt to escape by overcoming the desorption barrier.

Most of the time, this state will decay to its starting point by passing back the Br atom. When an etching event does occur, it is accompanied by the transfer of the now-unpaired bystander Si atom onto the terrace. This activity creates a dimer vacancy and provides Si for regrowth on the terrace.

Having established that dimer vacancies form, that Si atoms move onto the terrace and that $SiBr_2$ desorbs, we can use STM to address another issue. Suppose that the rate of desorption is not as simply related to the formation of that $SiBr_2$ unit, its desorption and to the release of the bystander as outlined above. Suppose, instead, that this sequence of events is very unlikely because the desorption barrier is too high and the lifetime of the surface $SiBr_2$ unit is too short. Gilles de Wijs (Ecole Normale Supérieure de Lyon), Alessandro De Vita (Ecole Polytechnique Fédérale de Lausanne) and Annabella Selloni (University of Geneva)[14] have recently explored these issues, and have calculated the barrier and the lifetime. The key event, they suggest, is not the desorption of $SiBr_2$, but the escape of the bystander. That escape would strand the $SiBr_2$ unit in its attempting-to-desorb state and enable it to make many more attempts than it otherwise could.

Investigating the roles of the Si bystander atom and the $SiBr_2$ molecule goes to the heart of material removal and points to vacancy creation as a critical step. One way to test this vacancy-assisted desorption picture is to measure the rate of desorption from surfaces that have been dosed with Br and then heated. If direct desorption is the key, then the rate should increase steadily with Br coverage as $SiBr_2$ formation on the surface becomes more and more likely. If, on the other hand, escape of the bystander is the key, then the rate should go through a maximum at an intermediate coverage because having too much Br on the surface would prevent transfer of Si onto the surface.

Preliminary results indeed suggest that the maximum desorption yield occurs when the amount of halogen is about 75% of a monolayer. And they imply that saturating the surface reduces the etch rate, in contrast to what is generally assumed.

Studies of the etch patterns and their formation, growth and evolution under steady-state conditions make it possible to measure differences in the effective energy barriers for processes like those described above. Once a single vacancy is created on a terrace, it destabilizes its neighbors and vacancy growth will produce a linear vacancy or a branched vacancy. For a pit of, say, seven vacancies on a line, growth will result in either an eight-unit line or a branched structure—similar to the one depicted in figure 1c. Analyzing STM images quantitatively indicates that removal events favor linear growth over branching by a ratio of 70:30, implying that the two paths differ in energy by only 0.14 eV. Although energy differences of this amount are small compared to a desorption energy of about 3 eV, they are

sufficient to account for the patterns observed during etching.

Finally, studies with atomic resolution STM have also led to the conclusion that there is a previously unexpected bonding configuration for Br on Si(100) at high temperature. This configuration is significant, for it provides a new pathway for etching. The normal, lower-temperature pathway occurs under conditions where, at most, one Br atom bonds to each Si dangling bond. Raising the temperature to 900 K causes a phase transition to occur. In this high-temperature 3×1 phase, the Br concentration is higher than in etching at lower temperatures, and rows of $SiBr_2$ units alternate with dimer rows of SiBr.[3]

The high-resolution image in figure 6 shows the special morphology that results from the desorption of the rows of $SiBr_2$. Clearly evident are rows of missing atoms between Si dimer chains. Present, too, are rows of missing dimers that are produced by normal etching. The variation in the brightness along the dimer rows is correlated with the presence or absence of residual Br atoms.

Future views

The emphasis throughout this article has been on the dynamic character of the surface when it is being etched—the ways in which atoms hop from one site to another and steps change in shape, and especially how this dynamic nature is ultimately reflected in the etch morphologies. As noted in the introduction, it was not obvious at first that the surfaces of Si and GaAs could be imaged with a probe as sensitive to atomic structure (and so easily confused by disorder) as STM. It is likely that the protocols discussed here can be applied to other systems and the even more complex environments of assisted etching.

The authors gratefully acknowledge Cari Herrmann's help in preparing this article.

References

1. H. F. Winters, J. W. Coburn, Surf. Sci. Rep. **14**, 161 (1992), and references therein.
2. G. Binnig, H. Rohrer, Helv. Phys. Acta, **55**, 137 (1982).
3. J. H. Weaver, C. M. Aldao, in *Morphological Organization during Epitaxial Growth and Removal*, M. G. Lagally, Z. Zhang, eds., World Scientific Series on Directions of Condensed Matter Physics, World Scientific, Singapore, in press.
4. J. S. Villarrubia, J. J. Boland, Phys. Rev. Lett. **63**, 306 (1989).
5. J. C. Patrin, J. H. Weaver, Phys. Rev. B **48**, 17913 (1993).
6. X.-S. Wang, R. J. Pechman, J. H. Weaver, J. Vac. Sci. Technol. B **13**, 2031 (1995).
7. B.-Y. Han, J. H. Weaver, Phys. Rev. B (in press).
8. R. M. Tromp, R. J. Hamers, J. E. Demuth, Phys. Rev. Lett. **55**, 1303 (1985).
9. K. Takayanagi, Y. Tanishiro, M. Takahashi, S. Takahashi, J. Vac. Sci. Technol. A **3**, 1502 (1985).
10. J. J. Boland, J. S. Villarrubia, Phys. Rev. B **41**, 9865 (1990).
11. B. S. Itchkawitz, M. T. McEllistrem, J. J. Boland, Phys. Rev. Lett. **78**, 98 (1997).
12. R. J. Pechman, X.-S. Wang, J. H. Weaver, Phys. Rev. B **52**, 11412 (1995). B. S. Itchkawitz, M. T. McEllistrem, H. Grube, J. J. Boland. Surf. Sci. **385**, 281 (1997)
13. M. Fouchier, J. J. Boland. Phys. Rev. B **57**, 8997 (1998).
14. G. A. de Wijs, A. De Vita, A. Selloni, Phys. Rev. Lett. **78**, 4877 (1997). ■